Asian Pub. Corp.

www.asianpubs.org

ARTICLE

Synthesis and Influence of Feret Diameter on Particle Morphology of Activated Carbon Derived from Agrowastes

A.S. Jadhav[1,✉], G.T. Mohanraj[2,✉], S. Mayadevi[3] and A.N. Gokarn[3]

Asian Journal of Materials Chemistry

Volume: 3 Year: 2018
Issue: 1–2 Month: January–June
pp: 28–36
DOI: https://doi.org/10.14233/ajmc.2018.AJMC-P62

Received: 31 May 2018
Accepted: 15 June 2018
Published: 27 June 2018

ABSTRACT

In this work, activated carbon was produced by chemical activation with phosphoric acid of agricultural wastes such as Arecanut shell of 180 mesh. Activated carbon is produced at activation temperature of 400 ºC by slow pyrolysis. The BET surface area and iodine number surface area was calculated and compared. The FTIR spectrum showed the presence of activated carbon. Thermogravimetric analysis revealed that the activated carbon is thermally stable at 480 ºC. The SEM images showed the incorporation of activated carbon particles. Surface area plot shows the details of morphological change caused by feret diameter on iodine number surface area, iodine number, methylene blue number and acid adsorption value. These results proves that the feret diameter plays important role in selection of final activation temperature and impregnation ratio, and also important in determining the quality of activated carbon obtained.

KEYWORDS

Arecanut shell, Activated carbon, Phosphoric acid, Feret diameter.

INTRODUCTION

A good quality activated carbon should have low ash content as possible [1], suggests that the typical values of ash content should be in the range of 5-7 % and about 85-90% for carbon content. As the carbon content of activated carbon increase, the surface area also increases. High carbon content value is desired to achieve high surface area.

Activated charcoal produced from residues would reduce the pressure on forests since wood is also commonly used for this purpose [2]. Many agricultural byproducts such as coconut shell [3,4], grain sorghum [5], coffee bean husks [6], rubber wood sawdust [7], chestnut wood [8], have been discovered to be suitable precursors for activated carbon due to their high carbon and low ash contents. Agricultural wastes are considered to be a very important feedstock because of especially two facts: (a) they are renewable sources and (b) low cost materials.

Arecanut shell is not a consumable part and is usually discarded as waste. Arecanut shell has become important species since its demand for export has increased tremendously. To make better use of low-cost and abundant agricultural waste, it is proposed to convert Arecanut shell waste into activated

Author affiliations:

[1]Department of Chemical Engineering, AISSMS College of Engineering, Pune-411001, India
[2]Department of Chemical Engineering, Birla Institute of Technology, Mesra, Ranchi-835215, India
[3]Chemical Engineering & Process Development, CSIR-National Chemical Laboratory, Pune-411 008, India

✉To whom correspondence to be addressed:

E-mail: gtmohanraj@gmail.com, asj.paper@gmail.com

Available online at: http://ajmc.asianpubs.org

carbon. This conversion will address problems of unwanted agricultural wastes been converted into useful, value-added adsorbent and also the use of agriculture by products to represent potential source of filler which will largely address problems of waste management. However, not many studies have been reported on converting Arecanut shell into activated carbon.

In the present study, the optimal experimental conditions required to obtain adequate activated carbon with desirable properties in terms of carbon yield, BET surface area, iodine number surface area and ash content, methylene blue number, iodine number, ferets diameter which is critical in determining a good quality activated carbon is studied.

EXPERIMENTAL

Preparation of activated carbon: First preparation of activated carbon was performed in three batch sizes of 50, 100 and 300 g. Phosphoric acid chemically pure quality (Merck company, India) was used as activating agent. A known mass of activated agent was mixed with distilled water and biomass waste was impregnated in acidic solution. The amount of phosphoric acid solution used was adjusted to give a certain impregnation ratio (weight of activating agent/weight of raw material) of 1:1, 2:1, 3:1 and 4:1. The impregnated sample was kept for 24 h. After 24 h, the residual water was removed and kept in oven for 110 ºC. A weighed amount of impregnated samples was kept in muffle furnace for 400 ºC. The muffle furnace is purged with high purity nitrogen gas to avoid oxidation. Nitrogen flow was adjusted to 3 mL/ºC at 400 ºC. The activated carbon was subsequently removed from furnace and cooled to room temperature.

After activation of the samples, 3 M HCl used to remove the phosphoric acid compounds. The washed samples were dried at 110 ºC for 6 h in oven and then ground to form a porous carbon powder. The equipment was fabricated to hold the raw sample of 30 cm × 9 cm × 9 cm size as shown in Fig. 1.

Physical characterization of arecanut shell activated carbon: The pore structures of the resulting carbons were analyzed using N_2 adsorption and scanning electron microscope (SEM).

Scanning electron microscope: SEM images were recorded using Joel JSM 6390LV field emission SEM. A thin layer of platinum was sputter-coated on the samples for charge dissipation during FESEM imaging. The sputter coater (Eiko IB-5 Sputter Coater) was operated in argon atmosphere using a current of 6 mA for 3 min. The coated samples were then transferred to the SEM specimen chamber and observed at an accelerating voltage of 5 kV, eight spot size, four aperture and 15 mm working distance.

Surface chemistry characterization of arecanut shell activated carbon: The surface chemistry characterization of the activated carbon was performed with pH drift and Fourier transform infrared spectroscopy (FT-IR) to identify its surface functional groups both qualitatively and quantitatively.

pH drift method: This method was conducted to determine the pH_{PZC} of arecanut shell activated carbon. The point of zero charge/zero charge point/zero point charge (pH_{PZC}) is pH when the charge in the activated carbon surface is zero. The procedure of pH drift method can be described as: 50 mL of 0.01 N NaCl was added into a series of Erlenmeyer. Then, their pH values were adjusted in range between 2 and 12 with interval 0.1 using 0.01N HCl solution and 0.01N NaOH. pH of initial solutions were measured with pH meter and then noted as pH initial. After constant value of pH initial had been reached, 0.15 g of activated carbon sample was added into each Erlenmeyer and then shaken for 48 h. After 48 h, pH of solution was measured using pH meter and noted as pH final. pH_{PZC} of activated carbon sample is the point when pH initial = pH final.

Arecanut shell derived activated carbon shown low pH_{PZC} in range of 2.5-3.0 These low pH_{PZC} values are consistent with Boehm titration result, which show always the dominance of acidic group at the surface of activated carbons.

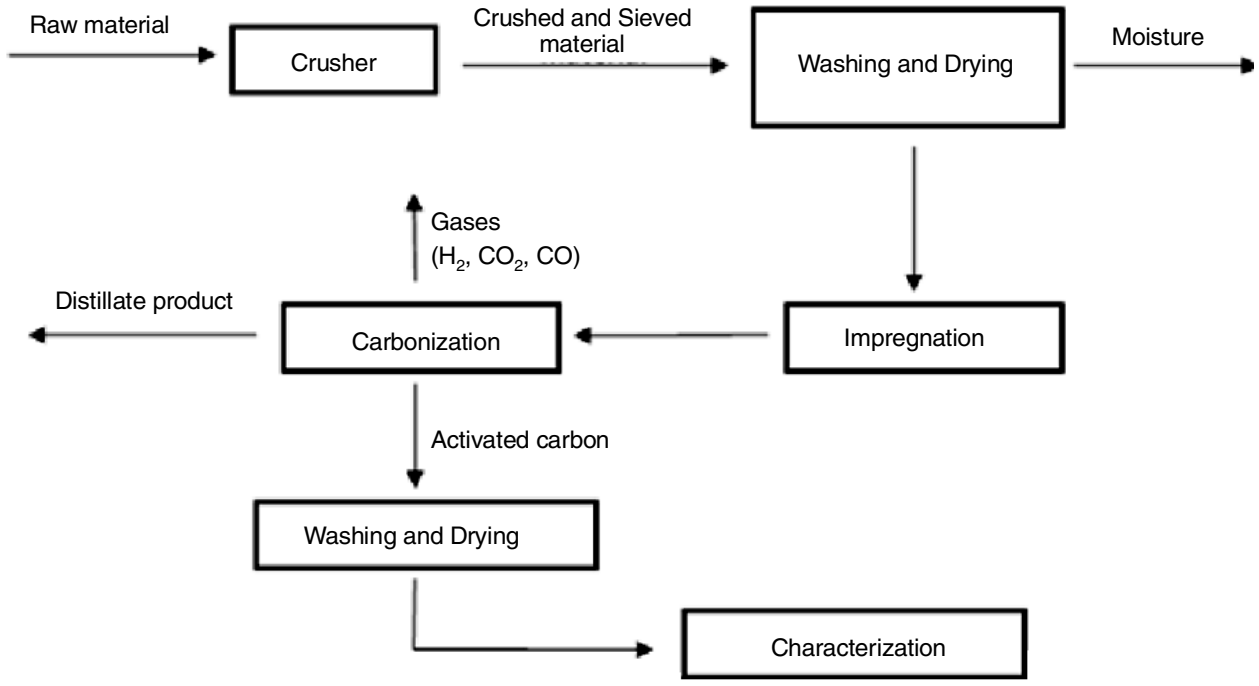

Fig. 1. Schematic diagram for preparation of activated carbon from arecanut shell

Boehm titration: The Boehm titration method can be described as: 0.5 g of activated carbon were placed to a series of flask which contain 50 mL of 0.05 N sodium bicarbonate, sodium carbonate, sodium hydroxide and hydrochloric acid. The flasks were sealed and shaken for 24 h. After 24 h, the solution is filtered and then 10 mL of each solution was pipetted to a flask and was titrated with 0.05 N NaOH and/or HCl, depending on the original solution used. The amount of acidic groups on the activated carbon is calculated under the assumption that NaOH neutralizes carboxylic, lactonic and phenolic groups. The number of surface basic sites is calculated from the amount of HCl that reacted with the carbon. The reaction between the reagents and the acidic oxygenated functional groups on the surface is based on the difference in acid/base strength. The strength of acidic groups is as follow: carboxyl > lactone > phenol [9].

Optimization of impregnation ratio: Table-1 depicted the yield obtained in percentage at 400 ºC by slow pyrolysis. Study was conducted at different impregnation ratio from 1:1 to 4:1 for different batch sizes of 50, 100 and 300 g. It is observed that yield increases uptill 3:1 impregnation ratio and decreases from 3:1 to 4:1, for batch sizes from 50,100 and 300 g. Thus impregnation ratio of 3:1 is referred as optimized impregnation ratio.

TABLE-1
YIELD OF BATCH SIZES

Sample	Yield % (50 g)	Yield % (100 g)	Yield % (300 g)
AS-PA-01 (1:1)	60.6	65.3	50.30
AS-PA-02 (1:2)	77.2	77.0	73.33
AS-PA-03 (1:3)	84.0	88.0	83.33
AS-PA-04 (1:4)	70.0	80.0	75.23

Optimization of pyrolysis temperature: Activation temperature optimization study was performed by performing runs at different temperatures (250, 300, 350 and 400 ºC). Runs were performed at these temperature because these temperature are known to be slow pyrolysis temperature. At 400 ºC yield remains constant for varying batch sizes. Thus temperature of 400 ºC was selected as optimized temperature condition for pyrolysis (Table-2).

TABLE-2
OPTIMIZATION OF PYROLYSIS TEMPERATURE

Experiment No.	Activation temperature (°C)	Yield (%)
1	300	60.5
2	375	71.0
3	400	84.0
4	425	84.0
5	450	84.0

Optimization of activation time: Activation time study is performed by taking run at different carbonization time from 30, 45, 60, 75 and 90 min.Yield at 90 min remained constant for activated carbon produced. Thus, 90 min is selected as optimized time condition for performing the final run of product. Hence, all experiments at different impregnation ratio were performed at 90 min (Table-3).

TABLE-3
OPTIMIZATION OF ACTIVATION TIME

Experiment No.	Activation time (min)	Yield (%)
1	30	63
2	45	68
3	60	75
4	75	79
5	90	88
6	95	88

Determination of methylene blue number: The methylene blue number (MBN) is a measure of mesoporosity (2-5 nm) present in activated carbon. Decolourizing power of carbon is expressed in terms of milligrams of methylene blue adsorbed by 1 g of activated carbon and is performed according to IS: 2230-1962.

$$\text{Decolourizing power} = \frac{15 \times V}{10 \times M}$$

where V is the volume of methylene blue solution (mL) consumed, M is the mass of material taken (g). The results are shown in Table-4.

TABLE-4
METHYLENE BLUE NUMBER (MBN)

Sample	MBN (50 g)	MBN (100 m)	MBN (300 g)
AS-PA-01 (1:1)	190	200	330
AS-PA- 02 (2:1)	200	300	345
AS-PA- 03 (3:1)	330	375	255
AS-PA- 03 (4:1)	275	290	225

Yield: The yield is defined as the ratio of final weight of the obtained product after washing and drying to the weight of dried precursor initially used. The yield of activated carbon was calculated based on the following equation:

$$\text{Yield} = \frac{\text{Weight of activated carbon after carbonization}}{\text{Weight of the raw material}} \times 100$$

Determination of adsorption of acid adsorption test: To a 10 mL of (acetic acid (50 mL) and water (400 mL)) sample and titrate it against 1N NaOH solution. Now added 10 g of activated carbon to 400 mL of sample. Stirred continuously for 0.5 h and withdraw 10 mL sample and titrate it with 1 N NaOH solution.

Determination of impregnation ratio: Impregnation ratio is defined as the ratio of weight of precursor to the chemical activating agent. Impregnation ratio is a key parameter for the preparation of activated carbon by chemical activation. Type of the chemical used and effect of impregnation ratio on various properties of prepared samples were explored in this section

$$\text{Impregnition ratio} = \frac{N \times \text{Weight of precursor } (W_1)}{\%\ \text{Purity of chemical activating agent}}$$

where N is the ratio number and W_1 is the weight of biomass sample

Determination of iodine number: The iodine number (IN) is a relative indicator of porosity in an activated carbon. It is a measure of micropore content of activated carbon (up to 2 nm). The iodine number is determined according to ASTM D4607-94 method. The iodine number is defined as the milligrams of

iodine adsorbed by 1.0 g of carbon, when the iodine concentration of the filtrate is 0.02 N (0.02 mol/L). Adsorption of iodine from an aqueous solution has been used to indicate absorptive capacity.

Iodine Number (Dry basis) =
F (mg of I_2 at outset – mg of I_2 at end of test)

where F is the filterate normality (N) = VN/50, V is colume of sodium thiosufate solution (mL) and N is the normality of sodium thiosulphate solution.

Iodine number surface area: Surface area per iodine atom (ω_I) is determined and correlated with the specific surface area measured by the method of low temperature argon adsorption (SBET) and the surface area (S_{IN}) measured by the iodine adsorption number (IN) for activated carbons.

Determination of iodine number surface area is one of the methods often adopted in the industry Thus:

$$S_I = \frac{IN \times 10^{-3} \times N \times \omega_I}{M_I}$$

Thermogravimetric analysis: The carbonization behaviour was measured by using thermobalance (DTG-60, Shimadzu Corporation) on the aspect of the weight loss behaviour. Temperature range is maintained from ambient to 1373 K. Heating rate range is from 0.01 to 60 K/min. Thermal study was performed on the activated carbon impregnated with the activating agents H_3PO_4. For each experimental run, a known weight of 6 ± 0.5 mg was placed on a platinum sample pan.

Fast fourier transform: It operates on a series of binned waveforms. A fast Fourier transform (FFT) is an algorithm that computes discrete Fourier transform (DFT) of a sequence or its inverse.

Determination of ferets diameter: It describes the maximal length straight-line that can be fitted into an object of interest, it is also known as maximum calliper. The longest distance between any two points along the selection boundary,

RESULTS AND DISCUSSION

Proximate analysis: The data (Table-5) revealed that the precursor used in this study has high carbon content approximately 75 % and low ash content about 6.4 % indicated that arecanut shell is suitable to be used as activated carbon precursor.

TABLE-5
PROXIMATE ANALYSIS OF ARECANUT SHELL

Material	Weight (%)
Ash	6.473
Moisture	11.46
Volatile matter	6.47
Fixed carbon	75.9
Total	100

Yield of activated carbon derived from arecanut shell: Fig. 2 depicted the effect of activation temperature and impregnation ratio on yield of activated carbon. The carbon yield was found to decrease with the increasing of impregnation ratio. The reaction of lignocellulosic with phosphoric acid begins as soon as the components are mixed, the acid first attacks hemicellulose and lignin because cellulose to be more resistant to

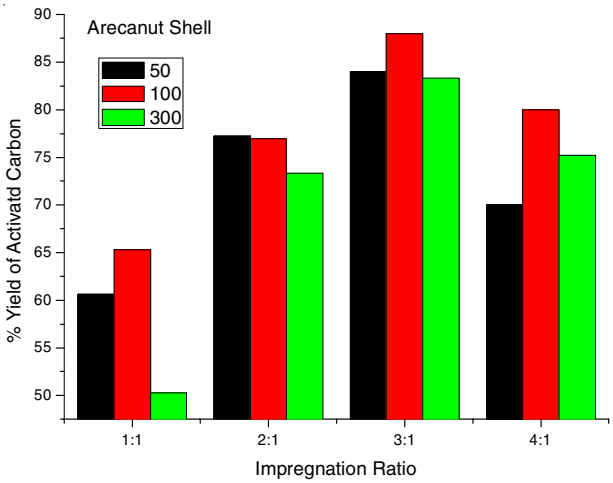

Fig. 2. Effect of impregnation ratio and activation temperature on yield of activated carbon

acid hydrolysis [10]. Here, acid will hydrolyze glycosidic linkages in lignocellulosic and leave aryl ether bond in lignin. These reactions are accompanied by further chemical transformations that include dehydration, degradation and condensation.

As the temperature increase, the aromatic condensation reactions also take place among the adjacent molecules, which result in the evolution of gaseous products from the hydroaromatic structure of carbonized char leading to decrease yield of carbon [11]. Impregnation ratio is another critical parameter that affects the quality of carbon. From Fig. 2, it is obvious that yield of carbon decreases as the impregnation ratio increase. The excess phosphoric acid will promote gasification of char and increased the total weight loss of carbon. The same result were also observed by other researchers [10-12].

Characterizing pore structure of activated carbon: The structural heterogeneity of activated carbon plays an important role in adsorption processes, have consequently been developed and applied for the characterization of this property. In this study, we used nitrogen adsorption, scanning electron microscopy to characterize carbon samples.

Effect of impregnition ratio on methylene blue number: Increase in methylene blue concentration showed no significant changes. This is due to the fact that with increased methylene blue concentration, the driving force for mass transfer also increases. At low concentrations, there will be unoccupied active sites on the adsorbent surface. Above optimal methylene blue concentration, the active sites required for the adsorption will lack. This retarded the overall methylene blue adsorption by activated carbon. Methylene blue number of greater than 400, indicates that the carbon is good for dye adsorption.

The methylene blue number increases uptill 3:1 ratio and decreases thereafter to 4:1 also methylene number for Arecanut shell is not greater than 400, thus it not suitable for dye adsorption (Fig. 3). Hence, suitability for dye adsorption made us to calculate the effect of impregnation ratio on iodine number which discussed further.

Effect of impregnation ratio on iodine number: Iodine number is the most fundamental parameter used to characterize activated carbon performance. It is a measure of micropore content of the activated carbon (0 to 20 Å or upto 2 nm) by adsorption of iodine from solution.

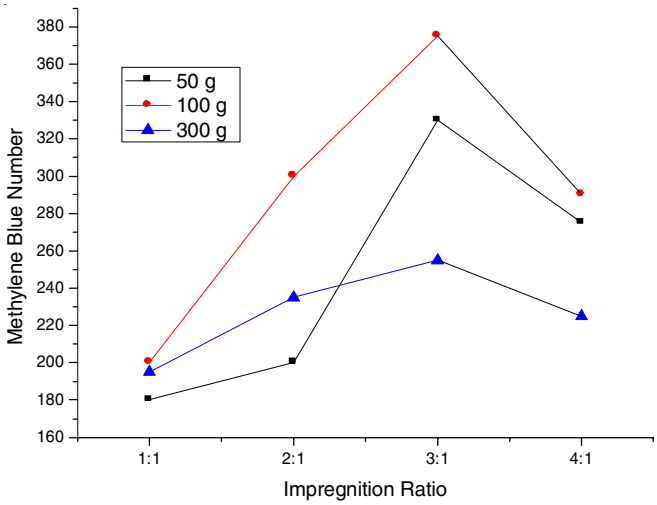

Fig. 3. Effect of Impregnation ratio on methylene blue number activated carbon

From the result of methylene blue value, it become necessary to know adsorptive capacity of iodine from an aqueous solution has been used to indicate absorptive capacity, iodine number increases for varying batch sizes from 50,100 and 300 g with different varying ratio of phosphorous acid (1:1-4:1) to activated carbon as iodine number increases there is increase in porosity of activated carbon. From Fig. 4, it is seen that iodine number decreases from ratio 3:1 to 4:1, for all batches indicated that degree of activation decreases.

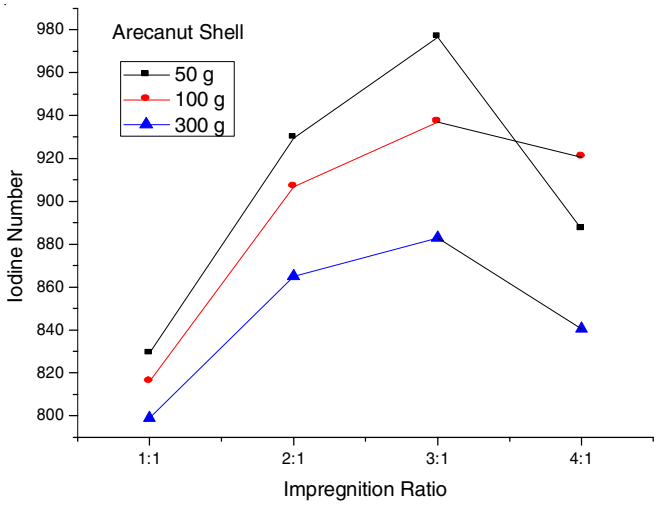

Fig. 4. Effect of impregnation ratio on iodine number

Effect of acid adsorption value: Water soluble matter and acid soluble matter give the information about the amount of impurities present in carbon which affect the quality of water. But in present analysis, the data showed that all carbons contain very low amount of impurities. Here as impregnation ratio increases from 1:1- 4:1, water soluble content increases uptill impregnation ratio of 3:1 and decreases from 3:1-4:1, for all batches from 50, 100 and 300 g. It observed that 300 g contains very less amount of impurities present as compared to 50 and 100 g (Fig. 5).

Thermogravimetric analysis: Thermogravimetric analysis of samples is presented in Fig. 6. Samples were analyzed by taking weight of sample: 0.01gm, Temperature range: 30-

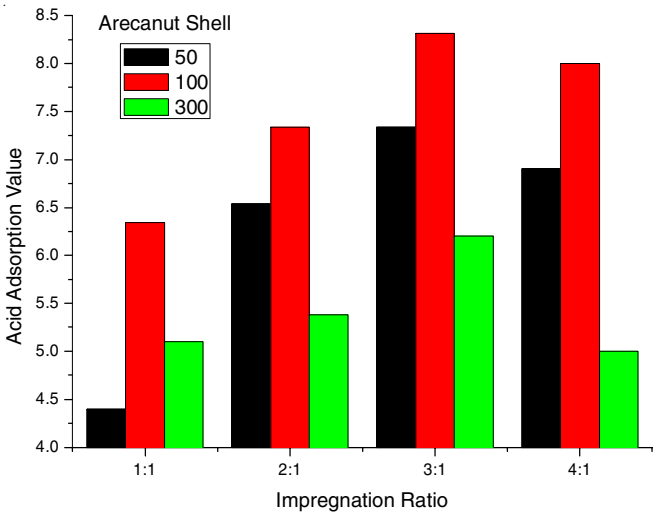

Fig. 5. Effect of impregnation ratio on acid adsorption

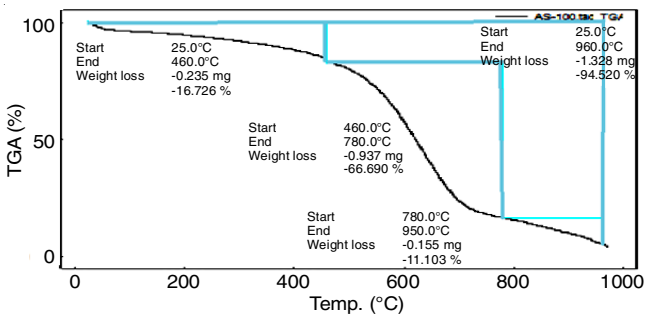

Fig. 6. TGA curve of arecanut shell

900°C and rate of heating: 10°C/min. 12% weight loss have been observed for Arecanut shell leaves weight loss of sample during analysis was 14 %. It is seen that activated carbon are thermally stable upto 150 ºC no appreciable weight loss. However, they show ed weight loss of 10 % in the first step, followed by weight loss of 11 % in second step (150-500 ºC) and major weight loss of 50 to 55 % form char residues 0-55 % in the steep third step, which ascribed to the thermal decomposition of polymeric backbone and carbonization of the fragments as well as activated carbon particles.

Effect of impregnation ratio on BET surface area: The BET does not predict the surface areas of microporous carbon. Thus it became necessary to calculate the surface are using iodine number. Determination of surface area of adsorbent is accomplished by using N_2 adsorption liquid, in which adsorbed N_2 molecules adhere on surface site as monolayer arecanut shell has the highest surface area. The surface area of different carbons follows the order: 50 g > 100 g > 300 g with increase in impregnation ratio.

Fig. 7 shows that the arecanut shell has the highest N_2 adsorption characteristics, while surface area increases from 1:1-3:1 and decreases from 3:1 to 4:1 for ratio 1:1 of 50 g surface area shows little variation, other than 100 and 300 g batch size. 300 g sample shows steady deviation .

Effect of impregnation ratio iodine number surface area: Determination of iodine adsorption number comprises the measurement of iodine amount in the adsorption layer of an activated carbon sample (in mg iodine/g adsorbent). Iodine number surface area is calculated to characterize the quality

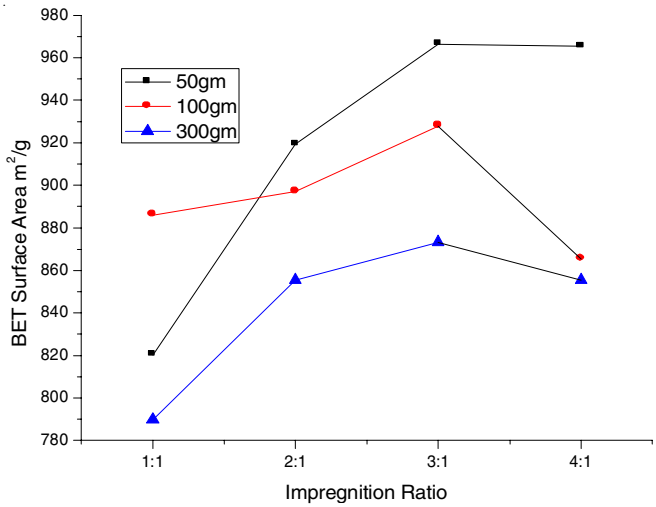

Fig. 7. Effect of impregnation ratio on BET surface area

of activated carbon. Table-6 depicted that iodine number surface area of arecanut shell, iodine number surface area increases initially for batch size of S_{IN} (50 g), S_{IN} (100 g) and S_{IN} (300 g) and for varying impregnation ratio from 1:1-3:1 and decreases from 3:1-4:1. This happens due to the change of bulk concentration results in the xomposition change of the interfacial layers, which induces mutual displacements of the solution components from the adsorbed layer [13]. During excess adsorption from the solution there are no unoccupied sites on the surface, which implies that same iodine amount occupies the same surface in different carbon samples.

TABLE-6
IODINE NUMBER SURFACE AREA OF 50, 100, 300 g
ACTIVATED CARBON DERIVED FROM ARECANUT SHELL

Sample	S_{IN} (50 g)	S_{IN} (100 g)	S_{IN} (300 g)
AS-PA-01 (1:1)	496.06	653.45	639.56
AS-PA-02 (2:1)	556.57	738.71	667.88
AS-PA-03 (3:1)	647.85	769.46	713.56
AS-PA-04 (4:1)	630.15	708.84	693.08

Comparison of external surfaces of resulting carbon using SEM: Scanning electron micrographs of the surface morphology of several samples of activated carbons are shown in Fig. 8. It is obvious that activated carbons produced at 400 ºC has cavities on their external surface. It can be predicted that the cavities on the carbon surfaces resulted from the evaporation of activating agent and in present case phosphoric acid during carbonization, leaves the space previously occupied by the activating agent. Similarly, fast Fourier transform (FFT)

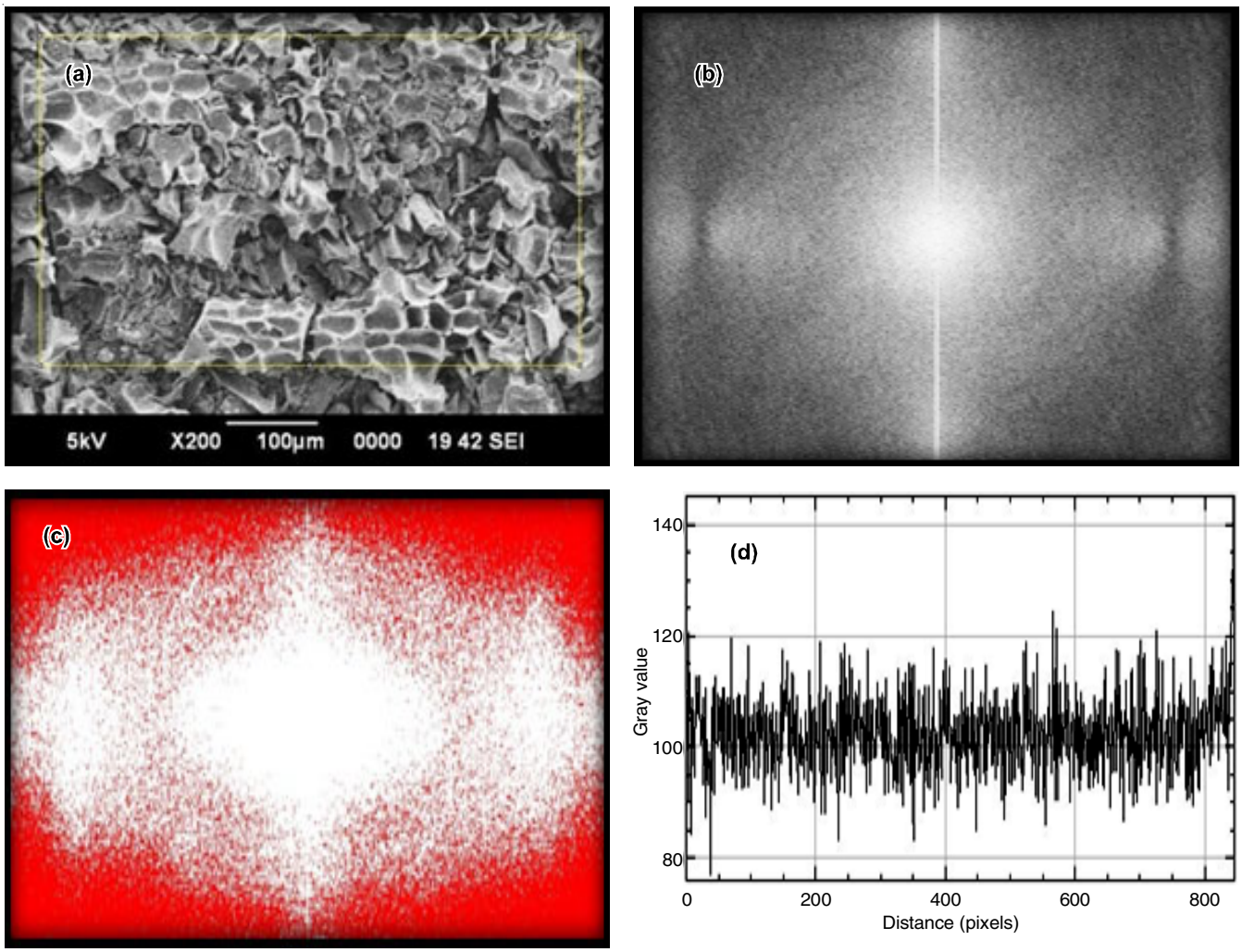

Fig. 8. SEM, FFT, threshold and profile plot of areca-nut shell particle; (a) SEM images activated carbons, (b) FFT image of SEM, (c) Threshold image of areca-nut shell particle distribution, d) Profile image of particle distribution

gives details of particle distribution of arecanut shell particles (Fig. 8).

Fourier transform infrared spectra: FTIR spectra of arecanut shell activated carbons with various impregnation ratios at each activation temperature are illustrated in Fig. 9. All the spectra show broad absorption band around 2999-2400 cm^{-1}. A peak around 1500 cm^{-1} shows the presence of stretching vibration of CO in ketones, aldehyde, lactone and carboxyl.

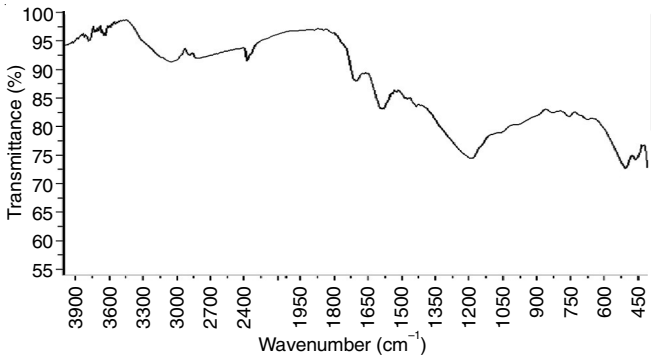

Fig. 9. Fourier transform infrafed spectra for arecanut shell activated carbon at activation temperature 400 °C

The presence of broad band around 2999-2400 cm^{-1} and peak around 1510 cm^{-1} indicates the presence of carboxylic acid [14,15]. A relative low intensity peak at wavenumber around 3100 cm^{-1} of broadband around 2999-2400 cm^{-1} may also represent OH stretching vibration in phenol. Very weak peak around 2900 cm^{-1} is C-H stretching vibration in methyl group [15]. A strong band at 1590 cm^{-1} can be ascribed to C-C aromatic ring stretching vibration enhanced by polar functional groups [8]. There is also a presence of broadband between 1300 and 1000 cm^{-1} with the strong band around 1200 cm^{-1} and a shoulder around 1080 cm^{-1}. According to Puziy *et al*. [8], the peak at 1220-1180 cm^{-1} may be ascribed to the stretching mode of hydrogen bonded P-O, O-C stretching vibrations in P-O-C linkage and P-OOH. The shoulder at 1080-1070 cm^{-1} can be ascribed to ionized linkage P^{+}–O^{-} in acid phosphate esters.

Surface images of arecanut shell captured by research microscope. Fig. 10a shows the original microscopic image of overall distribution of particles and Fig. 10b shows the section view of particle distribution.

Feret diameter: After performing all above analysis of particle size distribution, it became the necessity to calculate

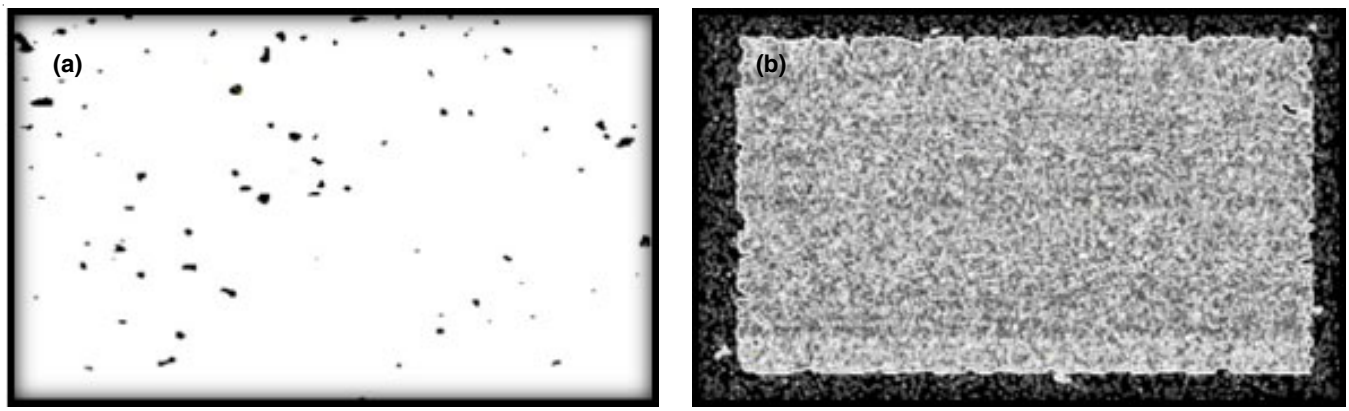

Fig. 10. Microscopic images of arecanut particle distribution (a) original microscopic image of particles (b) section view of particle distribution of arecanut shell

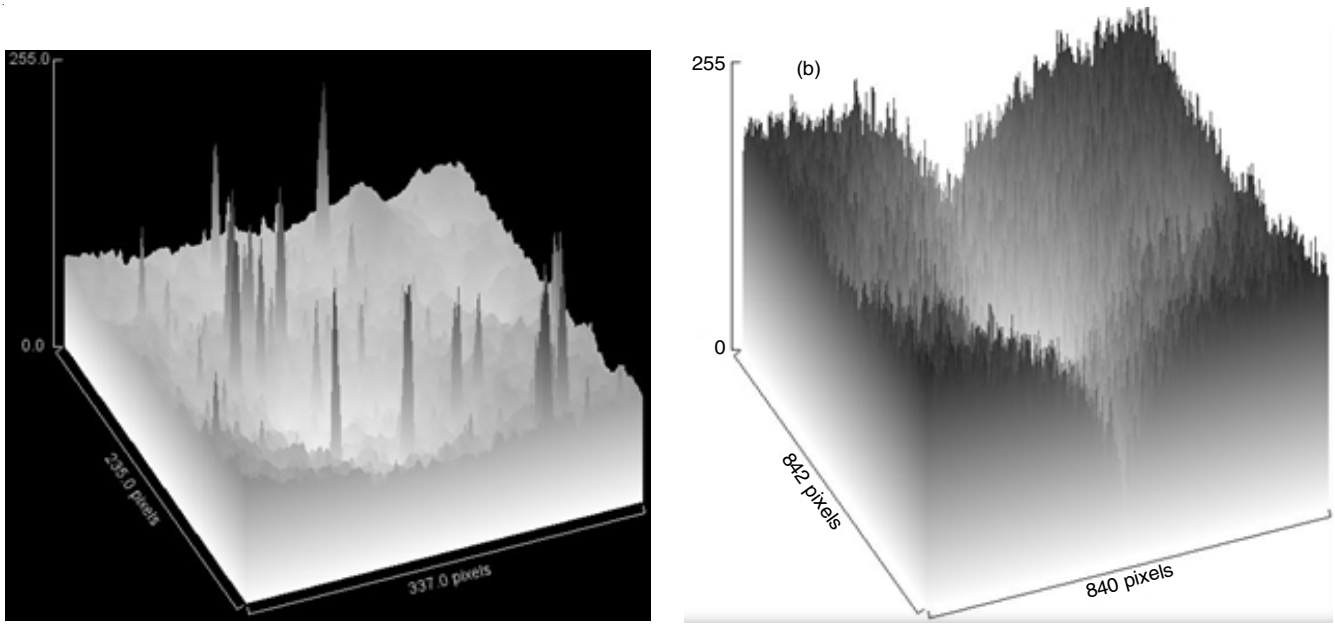

Fig. 11. Surface area plot images of (a) overall particle and (b) individual particle

the ferrate diameter. From Cauchy's theorem, it follows that for a 2D convex body, the Feret diameter averaged over all direction ⟨F⟩ is equal to the ratio of the object perimeter (P) and pi, *i.e.*, ⟨F⟩ = P/π. Perimeter of particle is calculated as =2.24 × 10^3. Therefore, feret diameter is found to be 8.00 × 10^2 (Fig. 11)

From Table-7, minimum feret diameter is 1 µm and feret diameter is measured from 2-6 µm and circularity is measured from 0.6-1. Circularity 1 defines particle is circular and less than 1 defines irregular shape. These circularity of particle help to increase the porosity and hence the adsorption rate of particle, which defines the solidity of particle. Thus, feret diameter influences the surface area of particle.

TABLE-7
FERET DIAMETER OF AVERAGE PARTICLES

Perim.	Circ.	Feret	Feret Angle	Min Feret	Solidity
11.899	1.000	5.385	21.801	3.000	0.889
5.657	1.000	2.828	45.000	2.000	0.857
7.657	1.000	3.606	146.310	2.000	1.000
5.657	1.000	2.828	135.000	2.000	1.000
10.485	1.000	4.472	153.435	3.000	0.857
5.657	1.000	2.828	45.000	2.000	0.857
12.485	1.000	5.000	126.870	4.000	0.897
7.657	1.000	3.606	123.690	2.000	1.000
18.728	1.000	7.616	156.801	5.000	0.889
5.657	1.000	2.828	45.000	2.000	0.857
18.728	0.967	7.280	105.945	5.000	0.885
7.657	1.000	3.606	146.310	2.000	1.000
22.971	0.476	9.849	23.962	3.905	0.656
9.899	1.000	4.472	26.565	3.000	0.800
12.485	0.887	5.385	68.199	3.000	0.846
5.657	1.000	2.828	135.000	2.000	1.000
4.243	1.000	2.236	153.435	1.000	1.000
28.385	0.577	10.000	126.870	7.000	0.747
9.071	1.000	4.243	45.000	3.000	0.875
9.899	0.898	4.123	165.964	3.000	0.737
9.071	1.000	4.243	45.000	3.000	0.941
9.657	1.000	4.243	135.000	3.000	1.000
5.657	1.000	2.828	45.000	2.000	0.857
9.899	1.000	4.472	26.565	3.000	0.857
13.899	1.000	5.831	120.964	4.000	0.889
10.485	1.000	4.472	153.435	3.000	0.909
13.314	1.000	5.385	158.199	4.000	0.889
46.527	0.720	16.553	115.017	11.586	0.805
16.728	1.000	6.708	63.435	5.000	0.885
4.243	1.000	2.236	153.435	1.000	1.000
17.314	0.545	7.280	74.055	3.000	0.722
18.728	0.860	6.708	116.565	6.000	0.857

Conclusion

Activated carbons were prepared from arecanut shell using phosphoric acid as chemical activating agent. The effect of impregnation ratio and activation temperature on pore structure and surface chemistry of resulting carbons were also studied. Optimiszed impregnation ratio for yield, methylene number, iodine number and acid adsorption value is 3:1. The surface chemistry was determined by Boehm titration method and FTIR to know the dominance of acid group. Thus, it can be concluded that carbon with well-developed pores are produced at activation temperature of 400 ºC. At constant activation temperature (at different impregnation ratio), the amount of acidic functional groups decreases while the basic surface groups of the carbon increases. This happens due to increase of yield uptill impregnation ratio 3:1 and decease from impregnation from 3:1 to 4:1. Thus impregnation ratio 3:1 is considered as optimized ratio. Iodine adsorption number comprises the measurement of iodine amount in adsorption layer of an activated carbon sample (in mg iodine/g adsorbent) methylene number value is below 400, depicted that arecanut shell derived activated carbon is not suitable for removal of dye particle. Thus, all carbonaceous materials can be converted into activated carbon, although the properties of the final product will be different, depending on the nature of the raw material used, the nature of activating agent and the conditions of carbonization and activation processes. Ferete diameter helps enhances the all characterization values and provides information about the adsorption application. Fast fourier transform (FFT) images helped to know particle applicability to reach the nanoscale value.

REFERENCES

1. S.D. Faust and O.M. Aly, Adsorption Processes for Water Treatment, Butterworth: Boston, MA, USA (1987).
2. Z. Hu and M.P. Srinivasan, Preparation of High-Surface-Area Activated Carbons from Coconut Shell, *Micropor Mesopor Mater.*, **27**, 11 (1999); https://doi.org/10.1016/S1387-1811(98)00183-8.
3. M. Sekar, V. Sakthi and S. Rengaraj, Kinetics and Equilibrium Adsorption Study of Lead(II) Onto Activated Carbon Prepared from Coconut Shell, *J. Colloid Interface Sci.*, **279**, 307 (2004); https://doi.org/10.1016/j.jcis.2004.06.042.
4. Y. Diao, W.P. Walawender and L.T. Fan, Activated Carbons Prepared from Phosphoric Acid Activation of Grain Sorghum, *Bioresour. Technol.*, **81**, 45 (2002); https://doi.org/10.1016/S0960-8524(01)00100-6.
5. M.C. Baquero, L. Giraldo, J.C. Moreno, F. Suarez-Garcia, A. Martinez-Alonso and J.M.D. Tascon, Activated Carbons by Pyrolysis of Coffee Bean Husks in Presence of Phosphoric Acid, *J. Anal. Appl. Pyrol.*, **70**, 779 (2003); https://doi.org/10.1016/S0165-2370(02)00180-8.
6. C. Srinivasakannan and M.Z.A. Bakar, Production of Activated Carbon from Rubber Wood Sawdust, *Biomass Bioenergy*, **27**, 89 (2004); https://doi.org/10.1016/j.biombioe.2003.11.002.
7. V. Gómez-Serrano, E.M. Cuerda-Correa, M.C. Fernández-González, M.F. Alexandre-Franco and A. Macías-García, Preparation of Activated Carbons from Chestnut Wood by Phosphoric Acid-Chemical Activation: Study of Microporosity and Fractal Dimension, *Mater. Lett.*, **59**, 846 (2005); https://doi.org/10.1016/j.matlet.2004.10.064.
8. A.M. Puziy, O.I. Poddubnaya, A. Martinez-Alonso, F. Suarez-Garcia and J.M.D. Tascon, Surface Chemistry of Phosphorus-Containing Carbons of Lignocellulosic Origin, *Carbon*, **43**, 2857 (2005); https://doi.org/10.1016/j.carbon.2005.06.014.
9. N. Wibowo, L. Setyadhi, D. Wibowo, J. Setiawan and S. Ismadji, Adsorption of Benzene and Toluene from Aqueous Solutions Onto Activated Carbon and its Acid and Heat Treated Forms: Influence of Surface Chemistry on Adsorption, *J. Hazard. Mater.*, **146**, 237 (2007); https://doi.org/10.1016/j.jhazmat.2006.12.011.
10. F. Rodriguez-Reinoso and M. Molina-Sabio, Activated Carbons from Lignocellulosic Materials by Chemical and/or Physical Activation: An Overview, *Carbon*, **30**, 1111 (1992); https://doi.org/10.1016/0008-6223(92)90143-K.
11. M. Jagtoyen and F. Derbyshire, Activated Carbons from Yellow Poplar and White Oak by H_3PO_4 Activation, *Carbon*, **36**, 1085 (1998); https://doi.org/10.1016/S0008-6223(98)00082-7.
12. H. Teng, T.S. Yeh and L.H. Hsu, Preparation of Activated Carbon from Bituminous Coal with Phosphoric Acid Activation, *Carbon*, **36**, 1387 (1998); https://doi.org/10.1016/S0008-6223(98)00127-4.

13. H. Jankowska, A. Swiatkowski and J. Choma, Active Carbon, Ellis Horwood Limited: West Sussex, England (1991).
14. Y. Guo and D.A. Rockstraw, Physical and Chemical Properties of Carbons Synthesized from Xylan, Cellulose and Kraft Lignin by H_3PO_4 Activation, *Carbon*, **44**, 1464 (2006); https://doi.org/10.1016/j.carbon.2005.12.002.
15. V. Boonamnuayvitaya, S. Sae-ung and W. Tanthapanichakoon, Preparation of Activated Carbons from Coffee Residue for the Adsorption of Formaldehyde, *Sep. Purif. Technol.*, **42**, 159 (2003); https://doi.org/10.1016/j.seppur.2004.07.007.